Journal of Applied Geophysics 135 (2016) 270–280

Contents lists available at ScienceDirect

Journal of Applied Geophysics

journal homepage: www.elsevier.com/locate/jappgeo

The influence of anisotropy on the apparent resistivity tensor: A model study

Annika Rödder *, Andreas Junge

Institute of Geosciences, Goethe University, Altenhöferallee1, 60438 Frankfurt am Main, Germany

ARTICLE INFO

Article history:
Received 11 March 2016
Received in revised form 13 October 2016
Accepted 17 October 2016
Available online 19 October 2016

Keywords:
Anisotropy
Apparent resistivity tensor
DCR
Modeling

ABSTRACT

The investigation of anisotropic structures within the subsurface using direct current resistivity methods (DCR) requires an array set up with measurements in different orientations. Displaying the data by the apparent resistivity tensor provides a powerful tool to easily identify anisotropic structures. In this study we present several characteristics of intrinsic electrical anisotropy and its effect on the apparent resistivity tensor. Above anisotropic anomalies the principle axes of the tensor exhibit a homogeneous pattern with orientation along the anisotropic strike and the aspect ratio related to the anisotropic properties of the medium. Contrary, outside the anomaly the ellipticity of the tensor and its apparent resistivity values are spatially highly variable depending on the location and the orientation of the source current dipole. Some of these features are in clear contrast to the behavior of the tensors above isotropic resistivity anomalies.

1. Introduction

Direct current methods are commonly used to solve hydrological, engineering or archeological questions. Besides the widely used collinear 2D multi-electrode measurements, 3D array measurements have been applied more often in the last years including cross-borehole or borehole to surface measurements (e.g. Ronczka et al. (2015), Martínez-Moreno et al. (2014), Negri et al. (2008)).

Isotropic 3D features or an anisotropic resistivity distribution cause directional dependent deviations in the current density and thus in the recorded voltages. In-line measurements along a profile do not provide any usable information about these properties. This methodological deficiency was remedied by Bibby (1977, 1986) introducing the apparent resistivity tensor which is explained in the next chapter in more detail. Considering one tensor invariant only is sufficient for some problems, e.g. model studies by Bibby and Hohmann (1993) show a strong influence of lateral resistivity contrasts on the tensors determinant. Varga et al. (2008) map an archeological excavation using some of the tensor invariants, while Bibby et al. (2002) apply large potential bipole separations and distances and high currents to analyze the resistivity distribution at large depth (2 km–3.5 km) below the Taupo Volcanic Zone in New Zealand.

As the apparent resistivity tensor contains directional dependent information, it is also suitable to study the strike of fracture zones. Santos et al. (2009) model fractures using a macroscopic anisotropy, which can be recognized in polar plots of each tensor element.

The presented model study shows the impact of an intrinsic anisotropy on the apparent resistivity tensor. Bibby and Hohmann (1993) and Wang et al. (2013) confine their studies to the influence of an intrinsic anisotropy on the determinant of apparent resistivity tensor. Expanding our study to other tensor invariants, resp. The elliptical representation of the apparent resistivity tensor (Bibby, 1977, 1986), we emphasize the apparent resistivity tensor's great potential for the detection and description of anisotropic resistivity distributions. Its use for the presentation of array field measurements can help to analyze the directional dependent properties of the subsurface, e.g. above fractured zones or shales.

2. The apparent resistivity tensor

Risk et al. (1970) describe the method of multiple source bipole–quadrupole measurements and Bibby (1977, 1986) introduces the apparent resistivity tensor at a site P related to a current injection at a remote site (Fig. 1) based on the general tensorial form of Ohm's law:

$$\underline{E} = \underline{\underline{\rho}}\ \underline{J} = \begin{pmatrix} \rho_{11} & \rho_{12} \\ \rho_{21} & \rho_{22} \end{pmatrix} \underline{J} \tag{1}$$

The current sources are located at AB and CD with the electric fields (E_{11}, E_{12}) and (E_{21}, E_{22}) resp. at P. The electric fields are estimated from the potential differences observed at MN and M′N′. The current densities $\underline{J}_{AB} = [J_{11}, J_{12}]$ and $\underline{J}_{CD} = [J_{21}, J_{22}]$ at P are calculated for an isotropic

* Corresponding author.
E-mail address: roedder@geophysik.uni-frankfurt.de (A. Rödder).

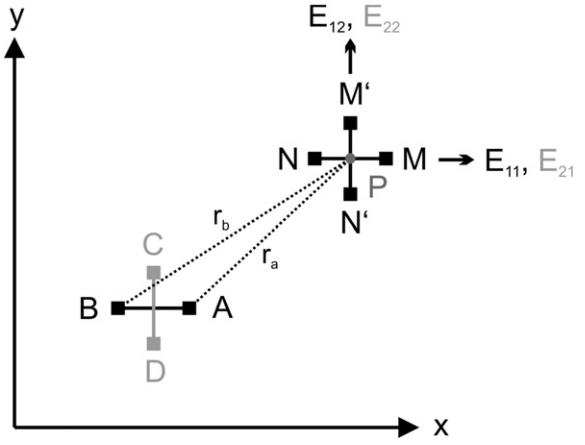

Fig. 1. Sketch of multiple source bipole–quadrupole DC resistivity measurement with current-bipole electrodes AB and CD and potential electrodes MN and M′N′ (modified after Bibby (1977)).

homogeneous halfspace. With Eq. (1) the apparent resistivity tensor is defined as

$$\underline{\underline{\rho}}_a = \begin{pmatrix} E_{11}J_{22}-E_{21}J_{12} & E_{21}J_{11}-E_{11}J_{21} \\ E_{12}J_{22}-E_{22}J_{12} & E_{22}J_{11}-E_{12}J_{21} \end{pmatrix} \cdot \left| \underline{J}_{AB} \times \underline{J}_{CD} \right|^{(-1)} \quad (2)$$

with the vector product $|\underline{J}_{AB} \times \underline{J}_{CD}| = J_{11}J_{22}-J_{12}J_{21}$. After Bibby (1977, 1986) this is a non-symmetric, second rank tensor also including the directional information. It can be described by three linearly independent rotational invariants:

$$P_1 = 0.5 \cdot \mathrm{trace}\left(\underline{\underline{\rho}}\right) = 0.5 \cdot (\rho_{11}+\rho_{22}) \quad (3)$$

$$P_2 = det\left(\underline{\underline{\rho}}\right)^{0.5} = (\rho_{11}\rho_{22}-\rho_{12}\rho_{21})^{0.5} \quad (4)$$

$$P_3 = 0.5 \cdot (\rho_{12}-\rho_{21}) \quad (5)$$

According to Bibby and Hohmann (1993), P_1 and P_2 are sensitive to lateral resistivity contrasts. Bibby (1977, 1986) display the apparent resistivity tensor by an ellipse. To calculate the ellipse parameters the tensor is split into a symmetrical and an asymmetrical part

$$\underline{\underline{\rho}}_a = \Pi_1 \begin{pmatrix} cos2\alpha & sin2\alpha \\ sin2\alpha & -cos2\alpha \end{pmatrix} + \Pi_2 \begin{pmatrix} cos2\beta & sin2\beta \\ sin2\beta & -cos2\beta \end{pmatrix} \quad (6)$$

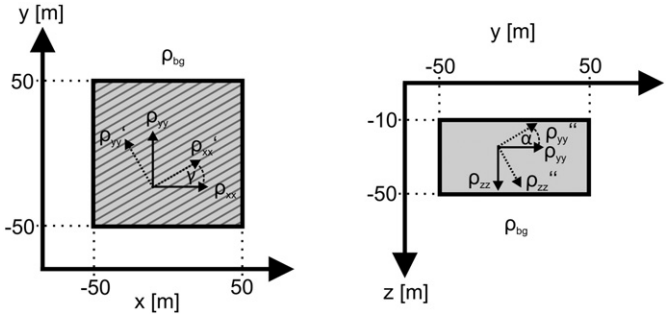

Fig. 2. Sketch of forward models. A cubic body with 100 m lateral extension and 40 m thickness is embedded at 10 m beneath the surface within an isotropic, homogenous background of 100 Ωm. The body's resistivity is varied according to Table 1.

Table 1
Main diagonal elements of the resistivity tensor and rotation angles of the cubic body.

	ρ_{diag}: $\rho_{xx}/\rho_{yy}/\rho_{zz}$ [Ωm]	$\alpha/\beta/\gamma$ [°]
Model A	1/1/1	0/0/0
Model B	1/100/1	0/0/0
Model C	1/100/1	0/0/30
Model D	1/100/1	30/0/0
Model E	1/100/100	0/0/0

with the rotational invariants $\Pi_1 = [P_1^2 + P_3^2 - P_2^2]^{0.5}$ and $\Pi_2 = [P_1^2 + P_3^3]^{0.5}$. The angle α is given by

$$\tan 2\alpha = (\rho_{12}+\rho_{21})/(\rho_{11}-\rho_{22.})$$

and the skewness β is defined as

$$\tan 2\beta = (\rho_{12}-\rho_{21})/(\rho_{11}-\rho_{22}) .$$

Then the ellipse's principal axes ρ_{min} and ρ_{max} result to

$$\rho_{\min} = \Pi_2 - \Pi_1, \quad (7)$$

$$\rho_{max} = \Pi_1 + \Pi_2 \quad (8)$$

and the rotation angle φ between the x-axis of the coordinate system and the major axis is

$$\phi = \alpha - \beta \quad (9)$$

In this paper we display the principal axes as normalized bars with their value color coded.

3. Model study

3.1. Model set up

The three dimensional (an-)isotropic models presented in this study are calculated using the AC/DC module of the FE program Comsol Multiphysics v.4.3a™ (Comsol, 2012a). The maximum area of interest is 500 m × 500 m × 200 m, however, the total model volume is 2 km × 2 km × 1 km to reduce the influence of the model boundaries. The model surfaces are defined as isolator, thus the current density's normal component equals zero at the boundaries. The electric potential declines to zero at the model boundaries except the surface (which is realized by the Comsol specific boundary condition *Electric Shielding*).

The unstructured tetrahedral grid is adapted to the gradient of the modeled fields such that the cells are finest close to the electrode positions and their size is increasing with distance. To keep the modeling simple, Comsol's AC/DC module default settings are used so that the non-surface boundary conditions are regarded as Dirichlet conditions (Comsol, 2012b). The implemented solver is an iterative conjugate gradient solver using a multigrid approach. This multigrid solver is combined by a successive over-relaxation (SOR) pre- and postsmoother and a direct MUMPS solver as coarse solver (Comsol, 2012a).

In average the models contain about 53,000 elements. On an i7-2600 CPU (3.40 GHz) machine with 16 GB RAM this yields a computing time of 168 s in the isotropic case and 169 s in the anisotropic case with two perpendicular current injections at one location.

To verify our models they were compared to the analytical solutions for an intrinsic anisotropic half-space by Das and Li (1996) and the results of Wang et al.'s (2013) forward code (Rödder-Löwer, 2016).

The presented models all contain a cubic anomaly embedded within a 100 Ωm half-space (Fig. 2). The cube's lateral extensions are 100 m in the horizontal and 40 m in the vertical direction and it is buried at 10 m depth.

The anomalies' resistivities are varied according to Table 1. It shows the values of the principal axis of the resistivity tensor and their Euler